Risk-Aware Optimal Control for Automated Overtaking With Safety Guarantees

Yulong Gao, Frank J. Jiang, Lihua Xie, *Fellow, IEEE*, and Karl Henrik Johansson, *Fellow, IEEE*

***Abstract*— This article proposes a solution to the overtaking control problem where an automated vehicle tries to overtake another vehicle with uncertain motion. Our solution allows the automated vehicle to robustly overtake a human-driven vehicle under certain assumptions. Uncertainty in the predicted motion makes the automated overtaking problem hard to solve due to feasibility issues that arise from the fact that the overtaken vehicle (e.g., a vehicle driven by an aggressive driver) may accelerate to prevent the overtaking maneuver. To counteract them, we introduce the weak assumption that the predicted velocity of the overtaken vehicle respects a supermartingale, meaning that its velocity is not increasing in expectation during the maneuver. We show that this formulation presents a natural notion of risk. Based on the martingale assumption, we perform a risk-aware reachability analysis by analytically characterizing the predicted collision probability. Then, we design a risk-aware optimal overtaking algorithm with guaranteed levels of collision avoidance. Finally, we illustrate the effectiveness of the proposed algorithm with a simulated example.**

***Index Terms*— Automated overtaking, automated vehicle, martingale, reachability analysis, risk-aware optimal control.**

I. Introduction

A. Motivation

OVERTAKING is a dangerous driving maneuver with both lateral and longitudinal movements. Many researchers believe that by developing an approach for safe, robust, and efficient overtaking, we will significantly progress the safety of automated vehicles [1], [2]. To this end, several existing works propose solutions for performing safe and efficient overtaking maneuvers [3]–[7]. However, these solutions all assume that the vehicle to be overtaken moves at a constant velocity. Under this assumption, overtaking can be formulated as a reference tracking problem or an optimal control problem. As long as the velocity of the overtaken vehicle is less than the speed limit and the prediction horizon is chosen appropriately, these problems do not encounter feasibility issues. Thus, the constant velocity assumption is a natural choice in many practical implementations. However, in this work, we consider overtaking vehicles that do not drive at a fixed velocity. We are motivated by human drivers who, depending on how they react to an overtaking, might change their velocities while being overtaken. To address these types of drivers, we present examples where if the vehicle being overtaken is changing its velocity, we can improve the overtaking compared to existing control laws.

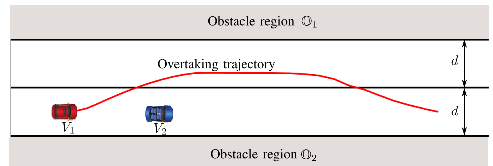

Fig. 1. Scenario where automated vehicle V_1 is overtaking the other vehicle V_2 on a road with two lanes.

B. Main Contributions

We study the process of overtaking a vehicle V_2 by an automated vehicle V_1, as shown in Fig. 1. The overtaking maneuver requires the automated vehicle to laterally move into an empty lane when it is safe to initiate the maneuver, longitudinally overtake V_2, and, finally, laterally merge back into the original lane in front of V_2. At each stage of the overtaking maneuver, many factors introduce uncertainty, which make the overtaking hard to perform robustly and safely [8].

The main objective of this work is to develop an algorithm for an overtaking control problem where an automated vehicle V_1 tries to overtake another vehicle V_2 with uncertain motion.

More specifically, we first propose a formulation for risk-aware reachability analysis based on martingale theory. We develop risk-aware reachable sets, which are subsets of traditional reachable sets. Risk-aware reachable sets are shown to admit predicted collision probabilities between V_1 and V_2. We estimate these collision probabilities analytically using the concentration inequality of martingale theory.

Manuscript received December 10, 2020; revised June 6, 2021; accepted August 20, 2021. Date of publication September 24, 2021; date of current version June 23, 2022. This work was supported in part by the Knut and Alice Wallenberg Foundation, in part by the Swedish Strategic Research Foundation, in part by the Swedish Research Council, and in part by the Wallenberg AI, Autonomous Systems and Software Program (WASP) funded by the Knut and Alice Wallenberg Foundation. Recommended by Associate Editor V. Zavala. *(Corresponding author: Yulong Gao.)*

Yulong Gao is with the Division of Decision and Control Systems, KTH Royal Institute of Technology, 11428 Stockholm, Sweden, and also with the School of Electrical and Electronic Engineering, Nanyang Technological University, Singapore 639798 (e-mail: yulongg@kth.se).

Frank J. Jiang is with the Division of Decision and Control Systems, KTH Royal Institute of Technology, 11428 Stockholm, Sweden (e-mail: frankji@kth.se).

Lihua Xie is with the School of Electrical and Electronic Engineering, Nanyang Technological University, Singapore 639798 (e-mail: elhxie@ntu.edu.sg).

Karl Henrik Johansson is with the Division of Decision and Control Systems, KTH Royal Institute of Technology, 11428 Stockholm, Sweden, and also with Digital Futures, 11428 Stockholm, Sweden (e-mail: kallej@kth.se).

Color versions of one or more figures in this article are available at https://doi.org/10.1109/TCST.2021.3112613.

Digital Object Identifier 10.1109/TCST.2021.3112613

Then, based on the proposed risk-aware reachability analysis, we design a risk-aware optimal overtaking algorithm. It is used to solve the overtaking problem in a receding-horizon manner. We provide sufficient conditions for the feasibility of the risk-aware optimal overtaking problem. In other words, by performing a safety check a step ahead of the execution of each control command, our algorithm can guarantee that the overtaking process is collision-free.

C. Literature Review

There is a significant body of work on automated overtaking under the assumption that the vehicle to be overtaken moves at a constant velocity. For example, model predictive control is used to track a reference overtaking trajectory in [3]–[5]. To handle collision avoidance, the overtaking problem is formulated as a mixed integer program in [6] and [7]. In [9], a constrained iterative linear quadratic regulator is used to efficiently solve the overtaking problem. The recent work [10] does not adopt the constant velocity assumption and considers measurement noises in the overtaking scenario, but no formal safety guarantees are provided.

Reachability analysis is a fundamental notion in systems and control theory [11], and is used to give formal safety guarantees for vehicle control [12], [13]. Robust approaches maintain strict guarantees that a system's state trajectory can be kept inside a safe tube by a feedback controller within a certain time horizon, despite bounded disturbances [14]. In [15]–[17], the authors formulate approaches for reachability-based automated overtaking for vehicles that overtake static obstacles using the opposing direction's lane. In [18], reachability analysis is incorporated into a model predictive controller for ensuring the safety of an automated vehicle when interacting with a human-driven vehicle. On the other hand, stochastic approaches guarantee that there will not be an unsafe trajectory within a certain time horizon for a given probability [19]. Stochastic reachability approaches can be beneficial, since they permit a tradeoff between collision probability and optimality, while avoiding decisions that are too conservative. However, the introduction of stochasticity often introduces the additional challenge of finding high-fidelity stochastic models. In [20], a Markov chain is used to model the uncertainty of other traffic participants and applied to probabilistic automated overtaking. Markov decision processes or partially observable Markov decision processes are used to model the stochasticity of human driving behavior in [21] and [22]. Such assumptions on human driving behaviors are quite strong. Another work [23] proposes an empirical method for generating approximate stochastic reachable sets for human-in-the-loop driving systems. However, in many overtaking scenarios, an automated vehicle will not have enough historical data to generate these empirical sets. In our recent work [24], we choose to use martingales to model the expected behavior of a human driver during overtaking. Our martingale assumption is weaker than the Markovian assumptions above. Less historical data is required to identify martingale-based models than is required to identify Markovian models, since Markovian models require the estimation of probability distributions. This article significantly generalizes the results in [24] by including a more detailed nonlinear vehicle model, a risk-aware optimal overtaking problem formulation, and a more general solution for solving this problem.

Historically, martingales are often applied to gambling or pricing problems since they efficiently model the lack of arbitrage [25]. In [26], how to use martingales is discussed in several classical stochastic control problems. In particular, supermartingales play an important role in stochastic stability and can be used for measures in risk theory. For example, a risk-neutral measure can also be called a martingale measure [27]. Moreover, in [28], the authors show that the multiportfolio time consistency of a dynamic multivariate risk measure is equivalent to a supermartingale property. In this article, under a supermartingale assumption, we propose risk-aware reachable sets and develop a risk-aware overtaking algorithm.

D. Organization

This article is structured as follows: in Section II, we introduce notation and preliminaries used throughout the article; in Section III, we detail the addressed problem; Section IV proposes risk-aware reachability analysis based on martingale theory; in Section V, a risk-aware optimal overtaking algorithm is presented while Section VI demonstrates the efficacy of our algorithm and compares our work with state-of-the-art; finally, Section VII concludes the article with a discussion on future work.

II. Notations and Preliminaries

A. Notations

We start by briefly clarifying different notation used in this work. Let $\mathbb{N}$ denote the set of nonnegative integers and $\mathbb{R}$ the set of real numbers. For some $q, s \in \mathbb{N}$ and $q < s$, let $\mathbb{N}_{[q,s]} = \{r \in \mathbb{N} \mid q \leq r \leq s\}$. For two sets $\mathbb{X}$ and $\mathbb{Y}$, $\mathbb{X} \oplus \mathbb{Y} = \{x + y \mid x \in \mathbb{X}, y \in \mathbb{Y}\}$. When $\leq$, $\geq$, $<$, and $>$ are applied to vectors, they are interpreted element-wise. For a set $\mathbb{X}$, $\mathcal{B}(\mathbb{X})$ denotes the Boral space of $\mathbb{X}$ and $\mathrm{cl}(\mathbb{X})$ the closure of $\mathbb{X}$. Pr denotes the probability and E the expectation.

B. Martingale Theory

Throughout this work, we will use the following definition and inequality from martingale theory. A supermartingale is a stochastic process for which the conditional expectation of future values given historical information is bounded from above by the current value. Formally, we define a supermartingale with the following definition.

Definition 1: [29] A discrete-time integrable stochastic process $\{X_i, i \in \mathbb{N}\}$ on a probability space $(\Omega, \mathcal{F}, \Pr)$, with a filtration $\{\mathcal{F}_i, i \in \mathbb{N}\}$ and $\mathcal{F}_i \subseteq \mathcal{F}$, is said to be a supermartingale if $\mathrm{E}[X_{i+1}|X_i] \leq X_i$, $\forall i \in \mathbb{N}$.

Due to the decreasing property of supermartingales, the following concentration inequality holds.

Lemma 1: [30] Consider a discrete-time supermartingale $\{X_i, i \in \mathbb{N}\}$ with a filtration $\{\mathcal{F}_i, i \in \mathbb{N}\}$ and $\mathcal{F}_i \subseteq \mathcal{F}$. If for

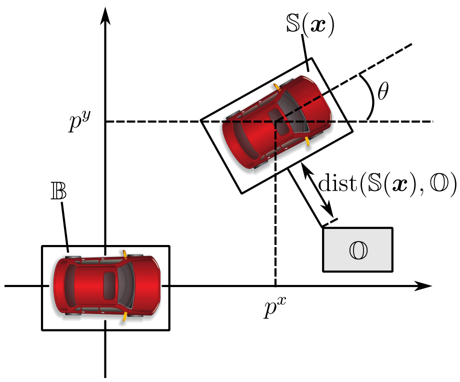

Fig. 2. Notation for obstacle avoidance.

all $i \in \mathbb{N}_{\geq 1}$, and some positive σ_i and M, $\text{Var}[X_i|\mathcal{F}_{i-1}] \leq \sigma_i^2$ and $X_i - \text{E}[X_i|X_{i-1}] \leq M$, then for all $\eta \geq 0$,

$$\Pr[X_i \geq X_0 + \eta] \leq \exp\left(-\frac{\eta^2}{2\left(\sum_{j=1}^{i} \sigma_j^2 + M\eta/3\right)}\right).$$

From Lemma 1, we can see that if a stochastic process is a supermartingale, the probability of the event $X_i \geq X_0 + \eta$ is upper bounded in terms of the variances σ_j, the step increment M, and the variable η. In this article, we assume that the predicted velocity of vehicle V_2 is a supermartingale (see Section IV-B). According to Lemma 1, there is only a small probability that the predicted velocity will become large. Thus, we can reasonably truncate the reachable sets by removing the small probability region. Furthermore, this small probability can be dictated by the exponential term in Lemma 1.

C. Vehicle Collision-Free Conditions

Consider a vehicle with state $\boldsymbol{x} = [p^x \ p^y \ \theta \ v]^T$, where (p^x, p^y) is the center of the rear axis (see Fig. 2), θ the heading angle, and v the velocity. For a given state $\boldsymbol{x}$, the occupancy of the vehicle is

$$\mathbb{S}(\boldsymbol{x}) = R(\boldsymbol{x})\mathbb{B} \oplus p(\boldsymbol{x}) \tag{1}$$

where $\mathbb{B} = \{z \in \mathbb{R}^2 \mid Gz \leq g\}$ is the initial rectangle occupied by the vehicle when the center of the rear axes is $[0; 0]$ and specified by $G \in \mathbb{R}^{2\times 2}$ and $g \in \mathbb{R}^2$, $R(\boldsymbol{x}) = [\cos\theta \ \ \sin\theta; -\sin\theta \ \ \cos\theta]$ the rotation matrix, and $p(\boldsymbol{x}) = [p^x; p^y]$.

Consider an obstacle $\mathbb{O} \subseteq \mathbb{R}^2$ of the form

$$\mathbb{O} = \left\{z \in \mathbb{R}^2 \mid Hz \leq h\right\} \tag{2}$$

where $H \in \mathbb{R}^{2\times 2}$ and $h \in \mathbb{R}^2$ are a known matrix and vector, respectively. Define the distance between $\mathbb{S}(\boldsymbol{x})$ and $\mathbb{O}$ as

$$\text{dist}(\mathbb{S}(\boldsymbol{x}), \mathbb{O}) = \min_{z\in\mathbb{R}^2}\{\|z\| \mid (\mathbb{S}(\boldsymbol{x}) \oplus z) \cap \mathbb{O} \neq \emptyset\}.$$

The following lemma provides a computationally useful way for checking if $\text{dist}(\mathbb{S}(\boldsymbol{x}), \mathbb{O}) > d$ for some $d > 0$.

Lemma 2: [31] For any $d > 0$, $\text{dist}(\mathbb{S}(\boldsymbol{x}), \mathbb{O}) > d$ if and only if there exist $\lambda \geq 0$ and $\mu \geq 0$ such that

$$\begin{cases} -g^T\mu + (Hp(\boldsymbol{x}) - h)^T\lambda > d \\ G^T\mu + R^T(\boldsymbol{x})H^T\lambda = 0 \\ \|H^T\lambda\| \leq 1. \end{cases}$$

The equivalent condition in Lemma 2 is derived using the dual problem of $\text{dist}(\mathbb{S}(\boldsymbol{x}), \mathbb{O})$. An important property of this equivalent condition is that all the decision variables are real numbers. This is different from the integer-based collision-avoidance formulation in the literature when taking into account the occupancy of the vehicle. The result of Lemma 2 will be used to reformulate the safety constraints on the overtaking vehicle in this article.

III. Problem Statement

We consider an overtaking scenario with an automated vehicle V_1 and another vehicle V_2 as illustrated in Fig. 1. Regard the two regions outside of the lanes as obstacles $\mathbb{O}_1$ and $\mathbb{O}_2$ of the form

$$\mathbb{O}_i = \left\{z \in \mathbb{R}^2 \mid H_i z \leq h_i\right\}, \quad i = 1, 2.$$

The width of each lane is d. The longitudinal velocity of each vehicle is bounded $v_{\min}^R \leq v^x \leq v_{\max}^R$.

A. Automated Vehicle V_1

We describe the dynamics of the automated vehicle V_1 using the following bicycle model:

$$\boldsymbol{x}_1(k+1) = f(\boldsymbol{x}_1(k), \boldsymbol{u}_1(k))$$

where

$$\boldsymbol{x}_1 = \begin{bmatrix} p_1^x \\ p_1^y \\ \theta_1 \\ v_1 \end{bmatrix}, \quad \boldsymbol{u}_1 = \begin{bmatrix} \psi_1 \\ a_1 \end{bmatrix}.$$

The longitudinal and lateral positions (p_1^x, p_1^y) correspond to the center of the rear axes, θ_1 is the yaw angle with respect to the x-axis, v_1 is the velocity with respect to the rear axes, ψ_1 is the steering angle and a_1 is the acceleration. The update map is

$$f(\boldsymbol{x}_1, \boldsymbol{u}_1) = \begin{bmatrix} p_1^x \\ p_1^y \\ \theta_1 \\ v_1 \end{bmatrix} + \delta \begin{bmatrix} v_1\cos\theta_1 \\ v_1\sin\theta_1 \\ L^{-1}v_1\tan\psi_1 \\ a_1 \end{bmatrix}$$

where L is the wheel base and δ the sampling period. An illustration of the bicycle model is given in Fig. 3.

There are physical limits on the state and control input

$$\begin{aligned} &\boldsymbol{x}_1(k) \in \mathbb{X}_1, \ \ \boldsymbol{u}_1(k) \in \mathbb{U}_1 \\ &\mathbb{X}_1 = \Big\{\boldsymbol{z} \in \mathbb{R}^4 \mid \boldsymbol{z} = \left[p^x, p^y, \theta, v\right]^T \\ &\qquad\quad 0 \leq p^y \leq 2d, \theta_{\min} \leq \theta \leq \theta_{\max} \\ &\qquad\quad v_{\min}^R \leq v\cos\theta \leq v_{\max}^R\Big\} \\ &\mathbb{U}_1 = \Big\{\boldsymbol{u} \in \mathbb{R}^2 \mid \boldsymbol{u} = [\psi \ \ a]^T, \\ &\qquad\quad \psi_{\min} \leq \psi \leq \psi_{\max}, a_{1,\min} \leq a \leq a_{1,\max}\Big\}. \end{aligned}$$

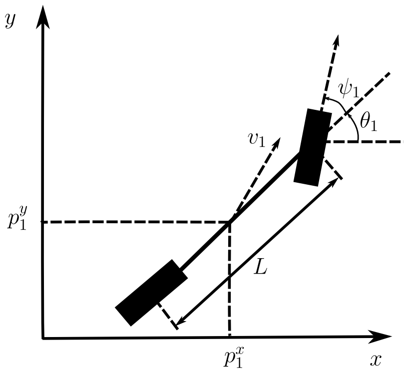

Fig. 3. Notation for bicycle model.

The occupancy of V_1 is

$$\mathbb{S}_1(\boldsymbol{x}_1(k)) = R(\boldsymbol{x}_1(k))\mathbb{B}_1 \oplus \begin{bmatrix} p_1^x(k) \\ p_1^y(k) \end{bmatrix}$$

where $\mathbb{B}_1 = \{z \in \mathbb{R}^2 \mid G_1 z \leq g_1\}$ is similarly defined as in Section II-C.

B. Overtaken Vehicle V_2

We specify the dynamics of the vehicle V_2 we want to overtake with the following linear model:

$$\boldsymbol{x}_2(k+1) = A_2\boldsymbol{x}_2(k) + B_2\boldsymbol{u}_2(k)$$

where

$$\boldsymbol{x}_2 = \begin{bmatrix} p_2^x \\ v_2^x \end{bmatrix}, \quad \boldsymbol{u}_2 = a_2^x$$
$$A_2 = \begin{bmatrix} 1 & \delta \\ 0 & 1 \end{bmatrix}, \quad B_2 = \begin{bmatrix} 0 \\ \delta \end{bmatrix}.$$

In particular, p_2^x, v_2^x, and a_2^x are the longitudinal position, velocity, and acceleration, respectively. During the overtaking process, we assume that V_2 stays in the same lane and maintains lateral position $p_2^y(k) = d/2$, $\forall k \in \mathbb{N}$.

Vehicle V_2 has the state and control input constraints

$$\boldsymbol{x}_2(k) \in \mathbb{X}_2, \quad \boldsymbol{u}_2(k) \in \mathbb{U}_2$$
$$\mathbb{X}_2 = \left\{ z \in \mathbb{R}^2 \;\middle|\; \begin{bmatrix} -\infty \\ v_{\text{min}}^R \end{bmatrix} \leq z \leq \begin{bmatrix} \infty \\ v_{\text{max}}^R \end{bmatrix} \right\}$$
$$\mathbb{U}_2 = \left\{ z \in \mathbb{R} \mid a_{2,\text{min}}^x \leq z \leq a_{2,\text{max}}^x \right\}.$$

The occupancy of V_2 is

$$\mathbb{S}_2(\boldsymbol{x}_2(k)) = \mathbb{B}_2 \oplus \begin{bmatrix} p_2^x(k) \\ d/2 \end{bmatrix}$$

where $\mathbb{B}_2 = \{z \in \mathbb{R}^2 \mid G_2 z \leq g_2\}$.

C. Problem

Our objective is to design a sequence of control inputs such that V_1 starts behind V_2 and ends in front of V_2 using the following maneuvers: lane-changing, lane-keeping, and merging. The constraint set $\mathbb{U}_2$ is known to the automated vehicle V_1. At each time step k, the automated vehicle V_1 can measure the states $\boldsymbol{x}_1(k)$ and $\boldsymbol{x}_2(k)$. Throughout the entire process, we maintain the following safety constraints: collision avoidance between V_1 and V_2, and collision avoidance between V_1 and $\mathbb{O}_i$, $i = 1, 2$.

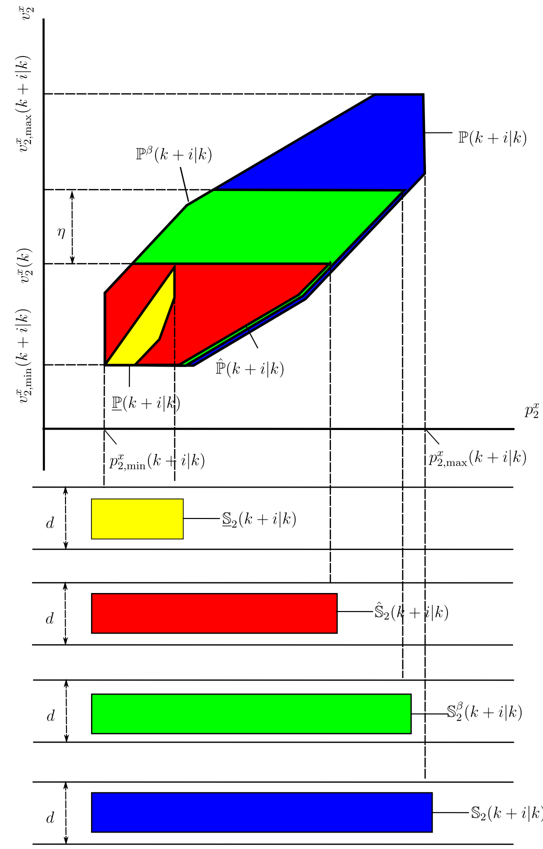

Fig. 4. Reachable sets for V_2 in the plane and their corresponding occupancy sets. (a) Blue: $\mathbb{P}(k+i|k)$ defined in (3) and $\mathbb{S}_2(k+i|k)$ defined in (4). (b) Green: $\mathbb{P}^\beta(k+i|k)$ defined in (7) and $\mathbb{S}_2^\beta(k+i|k)$ defined in (8). (c) Red: $\hat{\mathbb{P}}(k+i|k)$ defined in (11) and $\hat{\mathbb{S}}_2(k+i|k)$ defined in (9). (d) Yellow: $\underline{\mathbb{P}}(k+i|k)$ defined in (12) and $\underline{\mathbb{S}}_2(k+i|k)$ defined in (14). Here, $\beta(k+i|k) = 1-\exp(-(\eta^2/2(iM^2 + M\eta/3)))$, where $M = \max\{\delta|a_{2,\text{min}}^x|, \delta a_{2,\text{max}}^x\}$.

IV. Reachability Analysis

The reachable set of a vehicle is a subset of the state space that can be reached by the vehicle state through control actions. In this section, we introduce the reachable set and the risk-aware reachable set of vehicle V_2 and discuss some of their properties.

A. Reachable Set of Vehicle V_2

At time step k, $p_2^x(k)$ and $v_2^x(k)$ are the longitudinal position and velocity of V_2, respectively.

Definition 2: The reachable set predicted $i \in \mathbb{N}$ steps ahead at time step k is given by

$$\begin{cases} \mathbb{P}(k+i+1|k) = (A_2\mathbb{P}(k+i|k) \oplus B_2\mathbb{U}_2) \cap \mathbb{X}_2 \\ \mathbb{P}(k|k) = \{\boldsymbol{x}_2(k)\}. \end{cases} \tag{3}$$

Since the dynamics of V_2 is linear, the input constraint set $\mathbb{U}_2$ is a compact polyhedron and the state constraint set $\mathbb{X}_2$ is a polyhedron, the reachable sets in Definition 2 are compact polyhedra for all finite $i \in \mathbb{N}$. We show the set $\mathbb{P}(k+i|k)$ in blue in Fig. 4. Here, the x-axis denotes the position and the y-axis the velocity. The regions in different color are other reachable sets to be defined in the following. The rectangles below the x-axis are the corresponding occupancies also to be defined.

We define the projection of the reachable set on the longitudinal position as $\mathbb{P}_x(k+i|k) = \mathrm{Proj}_1\mathbb{P}(k+i|k)$ and the projection of the reachable set on the longitudinal velocity as $\mathbb{P}_v(k+i|k) = \mathrm{Proj}_2\mathbb{P}(k+i|k)$, where $\mathrm{Proj}_j(\mathbb{Q})$ denotes the projection of the set $\mathbb{Q}$ on the jth dimension.

It is noted that the set $\mathbb{P}(k+i|k)$ is a compact and convex set for all finite $i \in \mathbb{N}$. Furthermore, the sets $\mathbb{P}_x(k+i|k)$ and $\mathbb{P}_v(k+i|k)$ are closed intervals. For notational simplicity, let

$$\mathbb{P}_x(k+i|k) = \left[p^x_{2,\min}(k+i|k), p^x_{2,\max}(k+i|k)\right]$$
$$\mathbb{P}_v(k+i|k) = \left[v^x_{2,\min}(k+i|k), v^x_{2,\max}(k+i|k)\right].$$

These interval boundaries are also shown in Fig. 4. Denote all possible occupancies of V_2 corresponding to $\mathbb{P}_x(k+i|k)$ as $\mathbb{S}_2(k+i|k)$, that is

$$\mathbb{S}_2(k+i|k) = \left\{z \in \mathbb{R}^2 \mid z \in \mathbb{B}_2 \oplus \left[p^x_1(k); d/2\right] \; p^x_2 \in \mathbb{P}_x(k+i|k)\right\}. \quad (4)$$

It is a compact rectangle, which we denote as

$$\mathbb{S}_2(k+i|k) = \left\{z \in \mathbb{R}^2 \mid S(k+i|k)z \le s(k+i|k)\right\}$$

where $S(k+i|k)$ and $s(k+i|k)$ are a matrix and vector, respectively, with appropriate dimensions. The occupancy set $\mathbb{S}_2(k+i|k)$ is the blue rectangle below the x-axis in Fig. 4.

Intuitively, safe overtaking will be performed if the vehicle V_1 is able to plan an overtaking trajectory that avoids the reachable sets of V_2 as well as the obstacles $\mathbb{O}_1$ and $\mathbb{O}_2$. However, such a planner may encounter feasibility issues since the reachable sets of V_2 collect all possible future realizations, including reaching the speed limit to prevent the overtaking maneuver. In Section IV-B, we will show that if a supermartingale assumption is made on the predicted velocity of V_2, we will be able to introduce a risk to quantify the collision probability and truncate the reachable sets into risk-aware reachable sets to improve the planning feasibility.

B. Risk-Aware Reachable Set of Vehicle V_2

Let us next introduce the risk-aware reachable sets of V_2. Given any state $\boldsymbol{x}_2(k) \in \mathbb{X}_2$ at time step k, assume that the predicted velocity $\{v^x_2(k+i), i \in \mathbb{N}\}$ is a stochastic process with a filtration $\{\mathcal{B}(\mathbb{P}_v(k+i|k)), i \in \mathbb{N}\}$ on the probability space $([v^R_{\min}, v^R_{\max}], \mathcal{B}([v^R_{\min}, v^R_{\max}]), \mathrm{Pr})$. Then, the future state $\boldsymbol{x}_2(k+i|k)$, $i \ge 0$, is also a stochastic process.

We assume that the predicted velocity $v^x_2(k+i|k)$, $i \ge 0$, is a supermartingale, according to Definition 1. Consequently, we assume that for any state $\boldsymbol{x}_2(k) \in \mathbb{X}_2$ at time step k

$$\forall i \in \mathbb{N}, \quad \begin{cases} \boldsymbol{x}_2(k+i|k) \in \mathbb{P}(k+i|k), \\ \mathrm{E}\left[v^x_2(k+i+1|k) | v^x_2(k+i|k)\right] \le v^x_2(k+i|k). \end{cases}$$

Remark 1: The supermartingale assumption makes it possible to incorporate uncertain behaviors of human drivers [32]. By assuming that the predicted velocity of the overtaken vehicle V_2 respects a supermartingale, we generalize the common assumption in the literature that V_2 moves at a constant velocity.

Let $\boldsymbol{\alpha}(k) = \{\alpha(k+i|k), i \in \mathbb{N}\}$, where $0 \le \alpha(k+i|k) \le 1$, be the risk-coefficient sequence at time step k. This risk-coefficient sequence plays an important role in truncating the reachable sets and quantifies the collision probability after truncation. Under the supermartingale assumption, we define the sets

$$\mathbb{Y}^\alpha(k+i|k) = \left\{y \in \mathbb{R} \mid \mathrm{Pr}\left[\tilde{z} \ge v^x_2(k) + y\right] \le \alpha(k+i|k), \; \tilde{z} \in \mathbb{P}_v(k+i|k)\right\}$$
$$\mathbb{P}^\alpha_v(k+i|k) = \left\{v^x_2(k) + y \mid \left(v^x_2(k) + y\right) \in \mathbb{P}_v(k+i|k), \; y \in \mathbb{Y}^\alpha(k+i|k)\right\}$$

which corresponds to the set of velocity that V_2 can reach with probability less than $\alpha(k+i|k)$. Next let us consider how to compute the set $\mathbb{P}^\alpha_v(k+i|k)$.

Proposition 1: The set

$$\mathbb{P}^\alpha_v(k+i|k) = \left[\min\left\{v^x_2(k) + \eta, v^x_{2,\max}(k+i|k)\right\}, v^x_{2,\max}(k+i|k)\right] \quad (5)$$

where

$$\begin{cases} \eta = M\varrho/3 + \sqrt{M^2\varrho^2/9 + 2iM^2\varrho}, \\ M = \max\left\{\delta\left|a^x_{2,\min}\right|, \delta a^x_{2,\max}\right\}, \quad \varrho = -\ln(\alpha(k+i|k)). \end{cases} \quad (6)$$

Proof: Construct a filtration $\mathcal{F}_i = \mathcal{B}(\mathbb{P}_v(k+i|k))$. It follows from Popoviciu's inequality [33] that the variance of $v_2(k+i|k)$, conditioned on $v_2(k+i-1|k)$, is upper bounded by M^2, which implies that we can choose $\forall i \ge 1$, $\sigma_i^2 = M^2$ in the first condition of Lemma 1. From the constraint on the longitudinal acceleration of vehicle V_2

$$\left|v^x_2(k+i|k) - v^x_2(k+i-1|k)\right| \le M$$

thus the second condition of Lemma 1 also holds. Hence, (6) and (5) follows from Lemma 1 and setting:

$$\alpha(k+i|k) = \exp\left(-\frac{\eta^2}{2\left(\sum_{j=1}^{i}\sigma_j^2 + M\eta/3\right)}\right).$$

■

Remark 2: The parameter η in (6) corresponds to the minimal y in the set $\mathbb{Y}^\alpha(k+i|k)$ such that $v^x_2(k+y) \in \mathbb{P}_v(k+i|k)$. The set $\mathbb{P}^\alpha_v(k+i|k)$ is nonempty for all $0 \le \alpha(k+i|k) \le 1$.

Define another sequence $\boldsymbol{\beta}(k) = \{\beta(k+i|k), i \in \mathbb{N}\}$, where $\beta(k+i|k) = 1 - \alpha(k+i|k)$, $\forall i \in \mathbb{N}$. Let $\mathbb{P}^\beta_v(k+i|k) = \mathrm{cl}(\mathbb{P}_v(k+i|k) \setminus \mathbb{P}^\alpha_v(k+i|k))$, that is

$$\mathbb{P}^\beta_v(k+i|k) = \left[v^x_{2,\min}(k+i|k), \min\left\{v^x_2(k) + \eta, v^x_{2,\max}(k+i|k)\right\}\right].$$

Next we define the risk-aware reachable set.

Definition 3: The risk-aware reachable set for risk-coefficient $\alpha(k+i|k)$ is defined as

$$\mathbb{P}^\beta(k+i|k) = \left\{z \in \mathbb{R}^2 \mid z \in \mathbb{P}(k+i|k), \; \mathrm{Proj}_2(z) \in \mathbb{P}^\beta_v(k+i|k), \; \beta(k+i|k) = 1 - \alpha(k+i|k)\right\}. \quad (7)$$

Fig. 4 shows the set $\mathbb{P}^\beta(k+i|k)$ in green. It is noted that it is a subset of the reachable set $\mathbb{P}(k+i|k)$. We remark that the set $\mathbb{P}^\beta(k+i|k)$ depends on the risk-coefficient $\alpha(k+i|k)$: the smaller risk that is acceptable, the larger risk-aware reachable set.

The projection of the risk-aware reachable set on the longitudinal position is denoted by

$$\mathbb{P}_x^{\beta}(k+i|k) = \mathrm{Proj}_1\big(\mathbb{P}^{\beta}(k+i|k)\big).$$

Denote by $\mathbb{S}_2^{\beta}(k+i|k)$ all the possible occupancies of the vehicle V_2 corresponding to $\mathbb{P}_x^{\beta}(k+i|k)$, that is

$$\mathbb{S}_2^{\beta}(k+i|k) = \big\{z \in \mathbb{R}^2 \mid z \in \mathbb{B}_2 \oplus \big[p_2^x(k); d/2\big], \; p_2^x \in \mathbb{P}_x^{\beta}(k+i|k)\big\}. \quad (8)$$

The possible occupancy $\mathbb{S}_2^{\beta}(k+i|k)$ of V_2 is a compact rectangle, which can be written as

$$\mathbb{S}_2^{\beta}(k+i|k) = \big\{z \in \mathbb{R}^2 \mid S^{\beta}(k+i|k)z \le s^{\beta}(k+i|k)\big\}$$

where $S^{\beta}(k+i|k)$ and $s^{\beta}(k+i|k)$ are a matrix and a vector, respectively, with appropriate dimensions. The occupancy set $\mathbb{S}_2^{\beta}(k+i|k)$ is shown as the green rectangle below the x-axis in Fig. 4.

Remark 3: Another interpretation of the risk-aware reachable set is that

$$\begin{aligned}\mathbb{P}^{\beta}(k+i|k) = \big\{z \in \mathbb{R}^2 \mid\; & z \in \mathbb{P}(k+i|k), z = [z_1; z_2] \\ & \mathbb{Q} = \mathbb{B}_2 \oplus [z_1; d/2] \\ & \Pr(\mathbb{S}_1(k+i|k) \cap \mathbb{Q} \neq \emptyset) \le 1 - \beta(k+i|k)\big\}\end{aligned}$$

which corresponds to the predicted state set that the vehicle V_2 can reach such that the collision probability with the vehicle V_1 is no greater than $1-\beta(k+i|k)$ under the supermartingale assumption.

C. Geometrical Interpretation of Risk-Aware Reachable Sets

This section provides some geometrical interpretations of the reachable sets defined above and establishes the relation among them.

First of all, we show that the risk-aware reachable set $\mathbb{P}^{\beta}(k+i|k)$ scales with the coefficient $\beta(k+i|k) = 1-\alpha(k+i|k)$. If $\boldsymbol{\alpha}(k)$ satisfies $\alpha(k+i|k) = 0$, i.e., $\beta(k+i|k) = 1$, $\forall i \in \mathbb{N}$, the risk-aware reachable sets equal to the reachable sets, i.e., $\mathbb{P}^{\beta}(k+i|k) = \mathbb{P}(k+i|k)$ and $\mathbb{P}_x^{\beta}(k+i|k) = \mathbb{P}_x(k+i|k)$. In this case, complete safety is guaranteed. If $\boldsymbol{\alpha}(k)$ instead satisfies $\alpha(k+i|k) = 1$, i.e., $\beta(k+i|k) = 0$, $\forall i \in \mathbb{N}$, the parameter η in (6) is 0, thereby resulting in

$$\mathbb{P}_v^{\alpha}(k+i|k) = \big[v_2^x(k), v_{2,\max}^x(k+i|k)\big]$$
$$\mathbb{P}_v^{\beta}(k+i|k) = \big[v_{2,\min}^x(k+i|k), v_2^x(k)\big].$$

We define the reachable sets, the projection on the longitudinal position, and the occupancy set for $\alpha(k+i|k) = 1$, $\forall i \in \mathbb{N}$, as follows:

$$\hat{\mathbb{P}}(k+i|k) = \big\{z \in \mathbb{R}^2 \mid z \in \mathbb{P}(k+i|k) \; \mathrm{Proj}_2(z) \in \big[v_{2,\min}^x(k+i|k), v_2^x(k)\big]\big\} \quad (9)$$

$$\hat{\mathbb{P}}_x(k+i|k) = \mathrm{Proj}_1\big(\hat{\mathbb{P}}(k+i|k)\big) \quad (10)$$

$$\hat{\mathbb{S}}_2(k+i|k) = \big\{z \in \mathbb{R}^2 \mid z \in \mathbb{B}_2 \oplus \big[p_2^x(k); d/2\big] \; p_2^x \in \hat{\mathbb{P}}_x(k+i|k)\big\}. \quad (11)$$

These sets correspond to the red regions in Fig. 4. In this case, the automated overtaking problem is reduced to the scenario where we predict that the vehicle V_2 moves with an *average* velocity no greater than the current velocity $v_2^x(k)$.

For comparison with the control under the constant velocity assumption, we restrict the control set to $\underline{\mathbb{U}}_2 = [a_{2,\min}^x, 0]$, which implies that the predicted velocity cannot be greater than the measured velocity $v_2^x(k)$. Similarly, we define the reachable sets, the projection on the longitudinal position, and the occupancy set as follows:

$$\begin{cases}\underline{\mathbb{P}}(k+i+1|k) = \big(A_2\underline{\mathbb{P}}(k+i|k) \oplus B_2\underline{\mathbb{U}}_2\big) \cap \mathbb{X}_2 \\ \underline{\mathbb{P}}(k+i|k) = \{\boldsymbol{x}_2(k)\}\end{cases} \quad (12)$$

$$\underline{\mathbb{P}}_x(k+i|k) = \mathrm{Proj}_1\big(\bar{\mathbb{P}}(k+i|k)\big) \quad (13)$$

$$\underline{\mathbb{S}}_2(k+i|k) = \big\{z \in \mathbb{R}^2 \mid z \in \mathbb{B}_2 \oplus \big[p_2^x(k); d/2\big] \; p_2^x \in \bar{\mathbb{P}}_x(k+i|k)\big\}. \quad (14)$$

The set $\underline{\mathbb{P}}(k+i|k)$ represents the reachable sets when the vehicle V_2 moves with a velocity no greater than the current velocity, $v_2^x(k)$, i.e., the acceleration is no greater than 0. These sets correspond to the yellow regions in Fig. 4.

For ease of notation, we drop the time dependence of the sets. The relation among these sets is then given in the following proposition.

Proposition 2: The following set inclusion relations hold:

$$\underline{\mathbb{P}} \subseteq \hat{\mathbb{P}} \subseteq \mathbb{P}^{\beta} \subseteq \mathbb{P}$$
$$\underline{\mathbb{P}}_x \subseteq \hat{\mathbb{P}}_x \subseteq \mathbb{P}_x^{\beta} \subseteq \mathbb{P}_x$$
$$\underline{\mathbb{S}}_2 \subseteq \hat{\mathbb{S}}_2 \subseteq \mathbb{S}_2^{\beta} \subseteq \mathbb{S}_2.$$

Proof: Follows from the definitions. ■

Remark 4: A safe overtaking will be ensured if the vehicle V_1 is able to plan an overtaking trajectory that avoids the occupancy $\mathbb{S}_2$ induced by the reachable sets of V_2 as well as the obstacles $\mathbb{O}_1$ and $\mathbb{O}_2$. Intuitively, the less the reachable sets are truncated, the more safety is guaranteed. From the inclusion relation $\underline{\mathbb{S}}_2 \subseteq \hat{\mathbb{S}}_2 \subseteq \mathbb{S}_2^{\beta}$, we have that the risk-aware overtaking (even though the risk-coefficient sequence $\boldsymbol{\alpha}(k)$ is set to be 1, which corresponds to $\hat{\mathbb{S}}_2$) still provides more safety guarantee along the prediction horizon than control under the constant velocity assumption (which corresponds to $\underline{\mathbb{S}}_2$).

In Section V, we will treat the risk-coefficient sequence $\boldsymbol{\alpha}(k)$ as a decision variable to design a risk-aware overtaking controller.

V. Risk-Aware Optimal Overtaking Control

In this section, we formulate the risk-aware overtaking problem and then design a receding-horizon overtaking algorithm. We provide theoretical guarantee of this algorithm and discuss how to approximately solve the risk-aware overtaking problem to speed up computations.

A. Risk-Aware Optimal Overtaking

At time step k, the risk-aware overtaking problem can be formulated as $\mathcal{P}(\boldsymbol{x}_1(k), \boldsymbol{x}_2(k))$

$$\min_{T\in\mathbb{N},\boldsymbol{u}_1,\boldsymbol{\alpha}(k)} \max_{i\in\mathbb{N}_{[0,T]}} \alpha(k+i|k)$$

$$\text{s.t. } \forall i \in \mathbb{N}_{[0,T-1]}:$$

$$\boldsymbol{x}_1(k+i+1|k) = f(\boldsymbol{x}_1(k+i|k), \boldsymbol{u}_1(k+i|k)) \quad (15a)$$

$$\boldsymbol{u}_1(k+i|k) \in \mathbb{U}_1(k+i|k), \quad (15b)$$

$$\forall i \in \mathbb{N}_{[0,T]}:$$

$$\beta(k+i|k) = 1-\alpha(k+i|k) \quad (15c)$$

$$\boldsymbol{x}_1(k+i|k) \in \mathbb{X}_1(k+i|k) \quad (15d)$$

$$\mathbb{S}_1(\boldsymbol{x}_1(k+i|k)) \cap \mathbb{O}_j = \emptyset, \quad j=1,2 \quad (15e)$$

$$\mathbb{S}_1(\boldsymbol{x}_1(k+i|k)) \cap \mathbb{S}_2^{\beta}(k+i|k) = \emptyset \quad (15f)$$

$$\begin{cases} p_1^x(k+T|k) \geq p_{2,\max}^{x,\beta}(k+T|k) \\ p_1^y(k+T|k) = d/2 \\ \theta_1(k+T|k) = 0 \end{cases} \quad (15g)$$

where $p_{2,\max}^{x,\beta}(k+T|k) = \max\{z \mid z \in \mathbb{P}_x^{\beta}(k+T|k)\}$.

The optimization problem $\mathcal{P}(\boldsymbol{x}_1(k), \boldsymbol{x}_2(k))$ aims to minimize the worst case risk value over a horizon, subject to a feasible overtaking trajectory. The decision variables are the risk-coefficient sequence $\boldsymbol{\alpha}(k)$, the overtaking horizon T, and the control sequence $\{\boldsymbol{u}_1(k+i|k)\}_{i=0}^{T-1}$. The essence of this optimization problem is to tradeoff the feasibility of automated overtaking and the collision risk along the prediction horizon. In general, the overtaking problem encounters feasibility issues if the reachable set $\mathbb{P}(k+i|k)$ is used to set up potential collision regions. The introduction of a risk-coefficient sequence $\boldsymbol{\alpha}(k)$ could release a larger overtaking space, which improves feasibility. The problem $\mathcal{P}(\boldsymbol{x}_1(k), \boldsymbol{x}_2(k))$ looks for a minimal risk coefficient that makes the overtaking feasible.

In general, the min-max optimization problem $\mathcal{P}(\boldsymbol{x}_1(k), \boldsymbol{x}_2(k))$ is difficult to solve exactly, in particular in the presence of integer decision variable T. To remedy this, we solve the problems $\check{\mathcal{P}}(\boldsymbol{x}_1(k), \boldsymbol{x}_2(k), T_k)$ and $\hat{\mathcal{P}}(\boldsymbol{x}_1(k), \boldsymbol{x}_2(k), T_k)$ for approximating the solution to $\mathcal{P}(\boldsymbol{x}_1(k), \boldsymbol{x}_2(k))$, where $T_k \in \mathbb{N}$. The problem $\check{\mathcal{P}}(\boldsymbol{x}_1(k), \boldsymbol{x}_2(k), T_k)$ is simplified from $\mathcal{P}(\boldsymbol{x}_1(k), \boldsymbol{x}_2(k))$ by fixing the risk coefficients as 0 and the horizon as T_k, and is formulated as

$$\min_{\boldsymbol{u}_1} J(\boldsymbol{x}_1, \boldsymbol{u}_1, T_k)$$

$$\text{s.t. } (15a), (15b), (15d), (15e)$$

$$\forall i \in \mathbb{N}_{[0,T_k]}: \mathbb{S}_1(\boldsymbol{x}_1(k+i|k)) \cap \mathbb{S}_2(k+i|k) = \emptyset$$

$$\begin{cases} p_1^x(k+T_k|k) \geq \check{p}_{2,\max}^{x}(k+T_k|k) \\ p_1^y(k+T_k|k) = d/2 \\ \theta_1(k+T_k|k) = 0 \end{cases} \quad (16)$$

where $\check{p}_{2,\max}^{x}(k+T_k|k) = \max\{z \mid z \in \mathbb{P}_x(k+T_k|k)\}$. The problem $\hat{\mathcal{P}}(\boldsymbol{x}_1(k), \boldsymbol{x}_2(k), T_k)$ is derived from $\mathcal{P}(\boldsymbol{x}_1(k), \boldsymbol{x}_2(k))$ by fixing the risk coefficients to 1 and the horizon to T_k and is formulated as

$$\min_{\boldsymbol{u}_1} J(\boldsymbol{x}_1, \boldsymbol{u}_1, T_k)$$

$$\text{s.t. } (15a), (15b), (15d), (15e)$$

$$\forall i \in \mathbb{N}_{[0,T_k]}: \mathbb{S}_1(\boldsymbol{x}_1(k+i|k)) \cap \hat{\mathbb{S}}_2(k+i|k) = \emptyset$$

$$\begin{cases} p_1^x(k+T_k|k) \geq \hat{p}_{2,\max}^{x}(k+T_k|k) \\ p_1^y(k+T_k|k) = d/2 \\ \theta_1(k+T_k|k) = 0 \end{cases} \quad (17)$$

where $\hat{p}_{2,\max}^{x}(k+T_k|k) = \max\{z \mid z \in \hat{\mathbb{P}}_x(k+T_k|k)\}$. In the above problems, the cost function is

$$J(\boldsymbol{x}_1, \boldsymbol{u}_1, T_k) = \sum_{i=0}^{T_k-1} \left(\|\boldsymbol{x}_1(k+i|k)\|^2 + \|\boldsymbol{u}_1(k+i|k)\|^2\right) + \|\boldsymbol{x}_1(k+T_k|k)\|^2.$$

Intuitively, $\check{\mathcal{P}}(\boldsymbol{x}_1(k), \boldsymbol{x}_2(k), T_k)$ captures the overtaking in the most safe sense while $\hat{\mathcal{P}}(\boldsymbol{x}_1(k), \boldsymbol{x}_2(k), T_k)$ captures the overtaking in the most risky sense. We remark that: (1) either the feasibility of $\check{\mathcal{P}}(\boldsymbol{x}_1(k), \boldsymbol{x}_2(k), T_k)$ or the feasibility of $\hat{\mathcal{P}}(\boldsymbol{x}_1(k), \boldsymbol{x}_2(k), T_k)$ implies the feasibility of the original problem $\mathcal{P}(\boldsymbol{x}_1(k), \boldsymbol{x}_2(k))$; (2) the solutions to $\check{\mathcal{P}}(\boldsymbol{x}_1(k), \boldsymbol{x}_2(k), T_k)$ or $\hat{\mathcal{P}}(\boldsymbol{x}_1(k), \boldsymbol{x}_2(k), T_k)$ are suboptimal for $\mathcal{P}(\boldsymbol{x}_1(k), \boldsymbol{x}_2(k))$.

Next, let us show how to reformulate the safety constraints (15b) (16), and (17). Recall that $\mathbb{S}_2(k+i|k) = \{z \in \mathbb{R}^2 \mid S(k+i|k)z \leq s(k+i|k)\}$ and write $\hat{\mathbb{S}}_2(k+i|k) = \{z \in \mathbb{R}^2 \mid \hat{S}(k+i|k)z \leq \hat{s}(k+i|k)\}$. Thanks to Lemma 2, these three constraints can be equivalently rewritten as (18)–(20), as shown at the bottom of the next page. More specifically, the variables μ_1, μ_2, λ_1, and λ_2 are introduced for the constraint (15b), $\check{\mu}_3$ and $\check{\lambda}_3$ for (16), and $\hat{\mu}_3$ and $\hat{\lambda}_3$ for (17). To this end, we can see that the optimization problems $\check{\mathcal{P}}(\boldsymbol{x}_1(k), \boldsymbol{x}_2(k), T_k)$ and $\hat{\mathcal{P}}(\boldsymbol{x}_1(k), \boldsymbol{x}_2(k), T_k)$ are nonlinear programming problems.

B. Algorithm

The risk-aware optimal overtaking algorithm is shown in Algorithm 1. Here, TerInd is an indicator to determine whether the while loop (line 2) terminates or not. When it terminates, there are three possible outputs: {Successful, Infeasible, Undecidable}.

1) Initialization: At time $k=0$, we want to find a time horizon T_0 such that the optimization problem $\hat{\mathcal{P}}(\boldsymbol{x}_1(0), \boldsymbol{x}_2(0), T_0)$ is feasible. If the initial velocity of V_1 is greater than that of V_2 (i.e., $v_1^x(0) > v_2^x(0)$), then the time horizon T_0 is bounded by

$$\left\lfloor \frac{v_{\max}^R - v_1^x(0)}{\delta a_{1,\max}^x} \right\rfloor \leq T_0 \leq \left\lceil \frac{v_{\max}^R - v_2^x(0)}{\delta a_{2,\max}^x} \right\rceil.$$

The lower bound is the minimal time at which the velocity of V_1 reaches the velocity limit $v_{\max}^R$. The upper bound is the minimal time at which the velocity of V_2 reaches $v_{\max}^R$, i.e., the overtaking time of the worst-case scenario where V_2 prevents the overtaking. One can use the bisection method for searching T_0 by checking the feasibility of $\hat{\mathcal{P}}(\boldsymbol{x}_1(0), \boldsymbol{x}_2(0), T_0)$.

2) At Each Time Step k: We first check if the overtaking is completed (lines 7–10). If the longitudinal position $p_1^x(k)$ of V_1 is in front of V_2, the lateral position $p_1^y(k)$ of V_1 is $d/2$, and the heading angle $\theta_1(k)$ of V_1 is 0, then Algorithm 1 terminates with an output Successful.

If the overtaking is not completed, we solve the optimization problems for obtaining the control input. Let the time horizon $T_k = T_0 - k$. If the problem $\check{\mathcal{P}}(\boldsymbol{x}_1(k), \boldsymbol{x}_2(k), T_k)$ is feasible, solve $\check{\mathcal{P}}(\boldsymbol{x}_1(k), \boldsymbol{x}_2(k), T_k)$ (lines 12–14); otherwise, solve $\hat{\mathcal{P}}(\boldsymbol{x}_1(k), \boldsymbol{x}_2(k), T_k)$. If $\hat{\mathcal{P}}(\boldsymbol{x}_1(k), \boldsymbol{x}_2(k), T_k)$ is infeasible, stop with output Infeasible (lines 18–19); otherwise, implement $\boldsymbol{u}_1^*(k|k)$ which is picked up from the optimal solution of $\check{\mathcal{P}}(\boldsymbol{x}_1(k), \boldsymbol{x}_2(k), T_k)$ or $\hat{\mathcal{P}}(\boldsymbol{x}_1(k), \boldsymbol{x}_2(k), T_k)$ (lines 22–28).

In Algorithm 1, the resulting solution will not be directly implemented. As shown in line 22, we use $\mathbb{S}_1(\boldsymbol{x}_1(k+1|k)) \cap \mathbb{S}_2(k+1|k) = \emptyset$ to detect whether the first input can ensure safety at next time step. If $\mathbb{S}_1(\boldsymbol{x}_1(k+1|k)) \cap \mathbb{S}_2(k+1|k) \neq \emptyset$, it implies that there exist some possible states $\boldsymbol{x}_2(k+1)$ in $\mathbb{P}(k+1|k)$ such that $\mathbb{S}_1(\boldsymbol{x}_1(k+1|k)) \cap \mathbb{S}_2(\boldsymbol{x}_1(k+1)) \neq \emptyset$. In this case, Algorithm 1 terminates with an output Undecidable.

Algorithm 1 Risk-Aware Optimal Overtaking Algorithm

1: **Initialization**:
2: Set $k = 0$ and $\mathrm{TerInd} = 1$;
3: Find a time horizon T_0 such that $\hat{\mathcal{P}}(\boldsymbol{x}_1(0), \boldsymbol{x}_2(0), T_0)$ is feasible;
4: **Implementation**:
5: **while** TerInd **do**
6: Measure $\boldsymbol{x}_1(k)$ and $\boldsymbol{x}_2(k)$;
7: **if** $p_1^x(k) > p_2^x(k)$ & $p_1^y(k) = d/2$ & $\theta_1(k) = 0$ **then**
8: $\mathrm{TerInd} = 0$;
9: **Output**: Successful;
10: **else**
11: Let the time horizon $T_k = T_0 - k$;
12: **if** $\check{\mathcal{P}}(\boldsymbol{x}_1(k), \boldsymbol{x}_2(k), T_k)$ is feasible **then**
13: Solve $\check{\mathcal{P}}(\boldsymbol{x}_1(k), \boldsymbol{x}_2(k), T_k)$;
14: **else**
15: **if** $\hat{\mathcal{P}}(\boldsymbol{x}_1(k), \boldsymbol{x}_2(k), T_k)$ is feasible **then**
16: Solve $\hat{\mathcal{P}}(\boldsymbol{x}_1(k), \boldsymbol{x}_2(k), T_k)$;
17: **else**
18: $\mathrm{TerInd} = 0$;
19: **Output**: Infeasible;
20: **end if**
21: **end if**
22: **if** $\mathbb{S}_1(\boldsymbol{x}_1(k+1|k)) \cap \mathbb{S}_2(k+1|k) = \emptyset$ **then**
23: Implement $\boldsymbol{u}_1^*(k|k)$;
24: $k = k + 1$;
25: **else**
26: $\mathrm{TerInd} = 0$;
27: **Output**: Undecidable;
28: **end if**
29: **end if**
30: **end while**

C. Theoretical Results

In the following, we will provide some theoretical results. Under Algorithm 1, the overtaking maneuver is computed in a closed-loop manner. The closed-loop system for V_1 is

$$\boldsymbol{x}_1(k+1) = f\left(\boldsymbol{x}_1(k), \boldsymbol{u}_1^*(k|k)\right)$$

where $\boldsymbol{u}_1^*(k|k)$ is derived from the optimal solution of $\tilde{\mathcal{P}}(\boldsymbol{x}_1(k), \boldsymbol{x}_2(k))$.

Proposition 3 (Safety): If Algorithm 1 terminates with the output Successful, the closed-loop overtaking trajectory is collision-free.

Proof: In lines 22–28 of Algorithm 1, the collision avoidance between vehicles is guaranteed by $\mathbb{S}_1(\boldsymbol{x}_1(k+1|k)) \cap \mathbb{S}_2(k+1|k) = \emptyset$; in other works, the occupancy intersection of two vehicles at the next time step is empty. The feasibility of $\check{\mathcal{P}}(\boldsymbol{x}_1(k), \boldsymbol{x}_2(k), T_k)$ or $\hat{\mathcal{P}}(\boldsymbol{x}_1(k), \boldsymbol{x}_2(k), T_k)$ implies that under the control of $\boldsymbol{u}_1^*(k|k)$, there is no collision between V_1 and the obstacles $\mathbb{Q}_1$ and $\mathbb{O}_2$. If the output of Algorithm 1 is Successful, the closed-loop overtaking trajectory is collision-free throughout the whole overtaking process. ■

Proposition 4 (Successful Overtaking): By implementing Algorithm 1, if the optimization problem $\check{\mathcal{P}}(\boldsymbol{x}_1(k), \boldsymbol{x}_2(k), T_l)$ is feasible at some time step k, Algorithm 1 will terminate with the output Successful.

Proof: The feasibility of $\check{\mathcal{P}}(\boldsymbol{x}_1(k), \boldsymbol{x}_2(k), T_l)$ implies that there exist a time horizon T_k, a sequence of control inputs, $\{\boldsymbol{u}_1(k+i|k), i \in \mathbb{N}_{[0,T_k-1]}\}$, such that the constraints (15f)–(15g) are satisfied with $\alpha(k+i|k) = 0$, $\forall i \in \mathbb{N}_{[0,T_k]}$. At next time step $k+1$, with time horizon $T_k - 1$ and control inputs $\{\boldsymbol{u}_1(k+i+1|k), i \in \mathbb{N}_{[0,T_k-2]}\}$, the constraints (15f)–(15g) are still satisfied with

$$\forall j = 1, 2, \begin{cases} -g_1^T \mu_j(k+i|k) + \left(H_j p(\boldsymbol{x}_1(k+i|k)) - h_j\right)^T \lambda_j(k+i|k) > 0 \\ G_1^T \mu_j(k+i|k) + R^T(\boldsymbol{x}_1(k+i|k)) H_j^T \lambda_j(k+i|k) = 0 \\ \lambda_j(k+i|k) \geq 0, \mu_j(k+i|k) \geq 0, \|H_j^T \lambda_j(k+i|k)\| \leq 1 \end{cases} \tag{18}$$

$$\begin{cases} -g_1^T \check{\mu}_3(k+i|k) + (S(k+i|k) p(\boldsymbol{x}_1(k+i|k)) - s(k+i|k))^T \check{\lambda}_3(k+i|k) > 0 \\ G_1^T \check{\mu}_3(k+i|k) + R^T(\boldsymbol{x}_1(k+i|k)) S(k+i|k)^T \check{\lambda}_3(k+i|k) = 0 \\ \check{\lambda}_3(k+i|k) \geq 0, \check{\mu}_3(k+i|k) \geq 0, \|S(k+i|k)^T \check{\lambda}_3(k+i|k)\| \leq 1. \end{cases} \tag{19}$$

$$\begin{cases} -g_1^T \hat{\mu}_3(k+i|k) + \left(\hat{S}(k+i|k) p(\boldsymbol{x}_1(k+i|k)) - \hat{s}(k+i|k)\right)^T \hat{\lambda}_3(k+i|k) > 0 \\ G_1^T \hat{\mu}_3(k+i|k) + R^T(\boldsymbol{x}_1(k+i|k)) \hat{S}(k+i|k)^T \hat{\lambda}_3(k+i|k) = 0 \\ \hat{\lambda}_3(k+i|k) \geq 0, \hat{\mu}_3(k+i|k) \geq 0, \|\hat{S}(k+i|k)^T \hat{\lambda}_3(k+i|k)\| \leq 1. \end{cases} \tag{20}$$

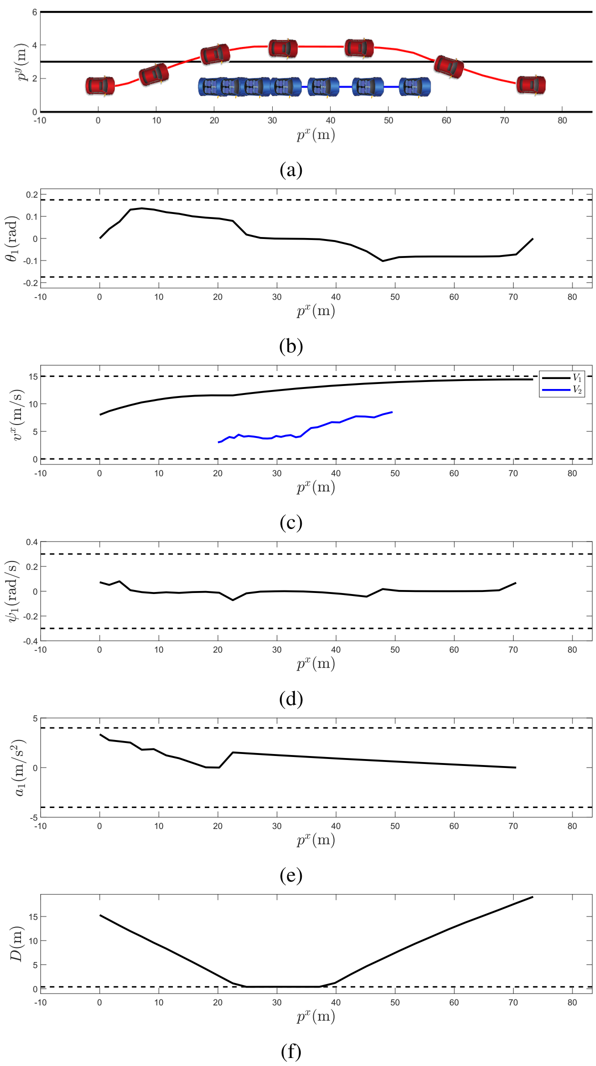

Fig. 5. **Successful overtaking**: (a) position of two vehicles. (b) Yaw angle of V_1. (c) Longitudinal velocities of two vehicles. (d) Steering angle of V_1. (e) Acceleration of V_1. (f) Distance between two vehicles.

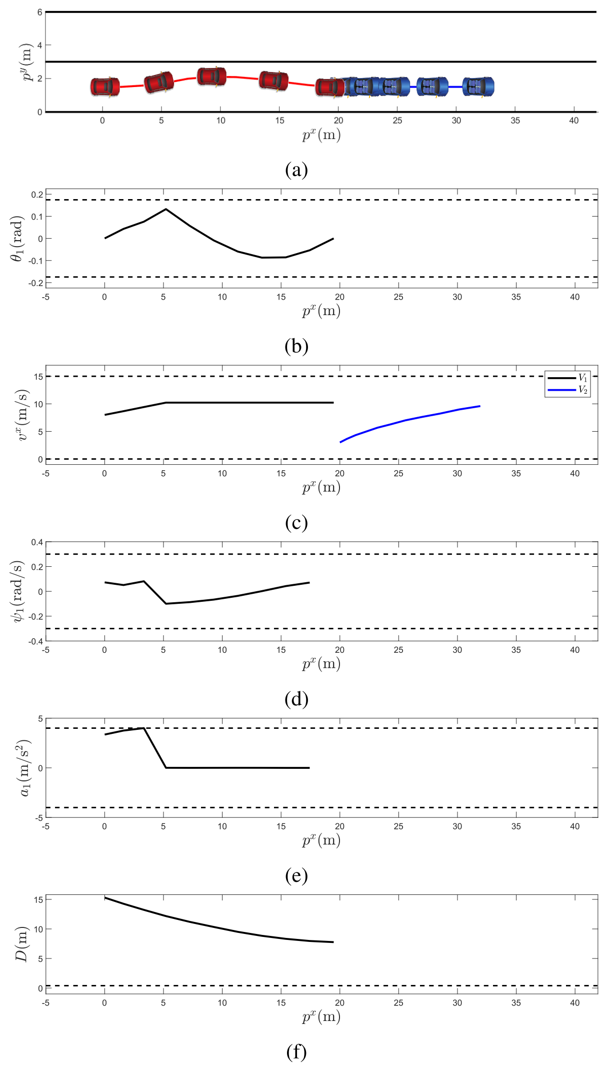

Fig. 6. **Unsuccessful overtaking**: (a) position of two vehicles. (b) Yaw angle of V_1. (c) Longitudinal velocities of two vehicles. (d) Steering angle of V_1. (e) Acceleration of V_1. (f) Distance between two vehicles.

$\alpha(k+1+i|k+1) = 0$, $\forall i \in \mathbb{N}_{[0,T_k-1]}$. By induction, it follows that the optimal solution of the problem $\mathcal{P}(\boldsymbol{x}_1(j), \boldsymbol{x}_2(j))$ is 0 for all $j \geq k$. We conclude that Algorithm 1 will terminate with the output Successful at most T_k steps. ■

Remark 5: Recall that the problem $\hat{\mathcal{P}}(\boldsymbol{x}_1(k), \boldsymbol{x}_2(k), T_l)$ is a simplified version of $\mathcal{P}(\boldsymbol{x}_1(k), \boldsymbol{x}_2(k))$ by fixing the risk coefficients to 1 and the horizon to T_k. Even though only $\hat{\mathcal{P}}(\boldsymbol{x}_1(k), \boldsymbol{x}_2(k), T_l)$ is feasible at the initial step $k = 0$, i.e., there exists collision risk along the prediction horizon, successful overtaking without collision is still possible. Intuitively, this is because uncertainty about future positions of V_2 is reduced significantly as time proceeds.

In the following, we give some tips for improving the online computational efficiency.

1) Both $\check{\mathcal{P}}(\boldsymbol{x}_1(k), \boldsymbol{x}_2(k), T_k)$ and $\hat{\mathcal{P}}(\boldsymbol{x}_1(k), \boldsymbol{x}_2(k), T_k)$ are nonlinear programming problems. Good initial guesses can improve the efficiency when solving nonlinear programming problems. In our case, one can choose the optimal solution $\{\boldsymbol{u}_1^*(k-1+i|k-1)\}_{i=1}^{T_{k-1}}$ at time step $k-1$ to be the initial guess at time k.
2) If $\check{\mathcal{P}}(\boldsymbol{x}_1(k), \boldsymbol{x}_2(k), T_k)$ is feasible at some step k, the sequence of the optimal solution $\{\boldsymbol{u}_1^*(k+i|k)\}_{i=1}^{T_k}$ can be directly implemented without solving the optimization problem for the remaining time steps. According to Proposition 4, this still ensures the safety of the overtaking.

VI. Numerical Evaluations

This section provides simulated case studies to demonstrate the effectiveness of our theoretical results. The following numerical experiments are run in MATLAB R2018b with ICLOCS2 toolbox [34], IPOPT toolbox [35], and MPT3 toolbox [36] on a Dell laptop with Windows 10, Intel i7-6600U CPU 2.80 GHz, and 16.0 GB RAM.

A. Successful and Unsuccessful Overtakings

The parameters used in the simulated example are listed in Table I, where l_i and w_i denote the length and width of

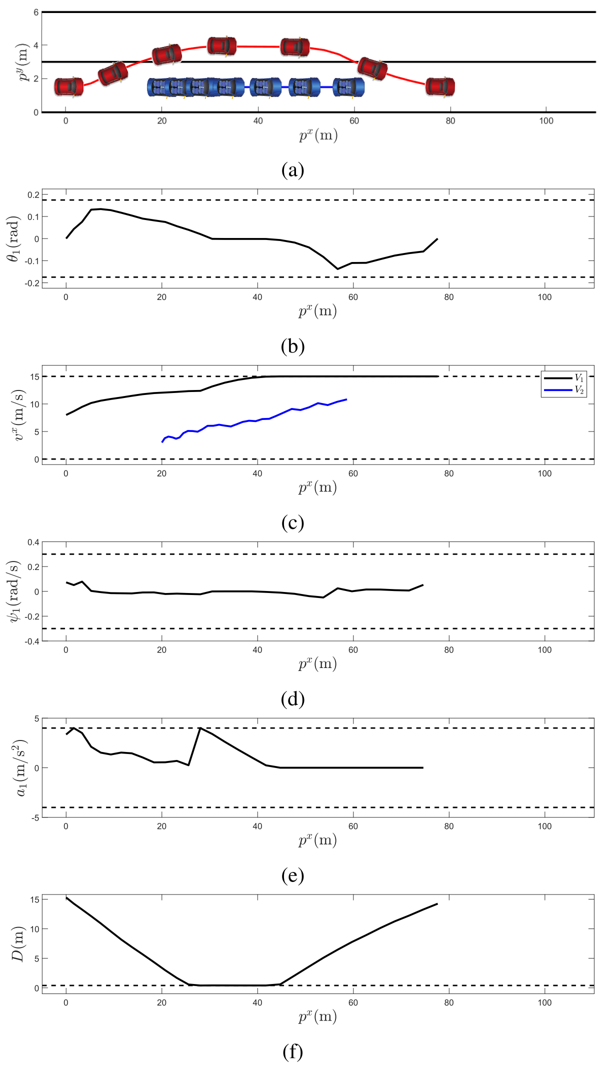

Fig. 7. **Risk-aware optimal overtaking**, first realization: (a) position of two vehicles. (b) Yaw angle of V_1. (c) Longitudinal velocities of two vehicles. (d) Steering angle of V_1. (e) Acceleration of V_1. (f) Distance between two vehicles.

TABLE I

CASE STUDY PARAMETERS

Lane	Vehicle 1	Vehicle 2
$v^R_{\min} = 0$ m/s	$\theta_{\min} = -\pi/18$ rad	$a^x_{2,\min} = -4$ m/s^2
$v^R_{\max} = 15$ m/s	$\theta_{\max} = \pi/18$ rad	$a^x_{2,\max} = 4$ m/s^2
$d = 5$ m	$a^x_{1,\min} = -4$ m/s^2	$l_2 = 4.7$ m
$\delta = 0.2$ s	$a^x_{1,\max} = 4$ m/s^2	$w_2 = 2$ m
	$\psi_{\min} = -0.6$ rad/s	
	$\psi_{\max} = 0.6$ rad/s	
	$L = 2.7$ m	
	$l_1 = 4.7$ m, $w_1 = 2$ m	

vehicle V_i, respectively. We choose the initial state: $\boldsymbol{x}_1(0) = [0; 1.5; 0; 8]$ and $\boldsymbol{x}_2(0) = [20; 3]$. A feasible time horizon T_0 at the initial time step is 31. To measure safety, we define the distance between the vehicles as

$$D(k) = \min_{\substack{z_1 \in \mathbb{S}_1(\boldsymbol{x}_1(k)) \\ z_2 \in \mathbb{S}_2(\boldsymbol{x}_2(k))}} \|z_1 - z_2\|.$$

In the following, we implement Algorithm 1 and provide two overtaking scenarios: one results in a Successful output while the other results in an Infeasible output.

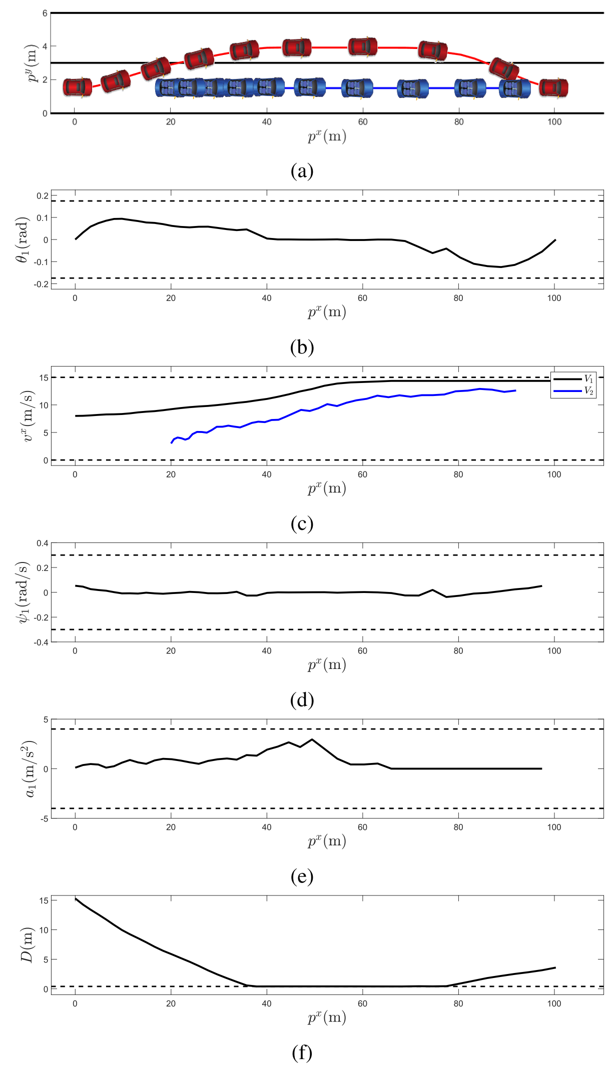

Fig. 8. **Receding horizon control with constant velocity prediction**, first realization: (a) position of two vehicles. (b) Yaw angle of V_1. (c) Longitudinal velocities of two vehicles. (d) Steering angle of V_1. (e) Acceleration of V_1. (f) Distance between two vehicles.

A successful overtaking attempt is shown in Fig. 5, where V_1 finally arrives in front of V_2 through a set of sequential maneuvers: lane-changing, lane-keeping, and merging. Fig. 5(a) shows the position trajectories of the two vehicles. In Fig. 5(b) and (c), we show the yaw angle of V_1 and the longitudinal velocities, respectively. Here, the longitudinal velocity of V_1 is $v_1(k)\cos\theta_1(k)$. It is noted that the longitudinal velocity of V_2 increases. Both yaw angle and longitudinal velocities satisfy their corresponding constraints. In Fig. 5(d) and (e), we show that the control inputs of the automated vehicle (steering angle and acceleration) satisfy the control input constraints. Furthermore, Fig. 5(f) shows that the collision avoidance between two vehicles is guaranteed.

An infeasible overtaking attempt is shown in Fig. 6. In Fig. 6(a), we show the position trajectories of two vehicles. In Fig. 6(b) and (c), we show the yaw angle of V_1 and longitudinal velocities of two vehicles, respectively. Both yaw angle and longitudinal velocities satisfy their corresponding constraints. Initially, since the problem $\hat{\mathcal{P}}$ is feasible, the

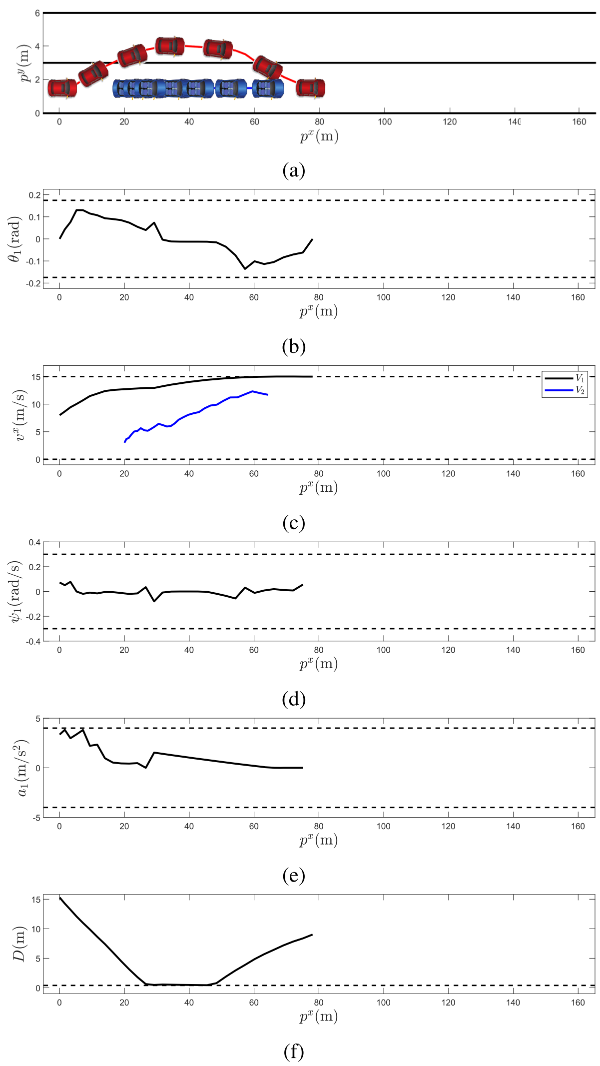

Fig. 9. **Risk-aware optimal overtaking**, second realization: (a) position of two vehicles. (b) Yaw angle of V_1. (c) Longitudinal velocities of two vehicles. (d) Steering angle of V_1. (e) Acceleration of V_1. (f) Distance between two vehicles.

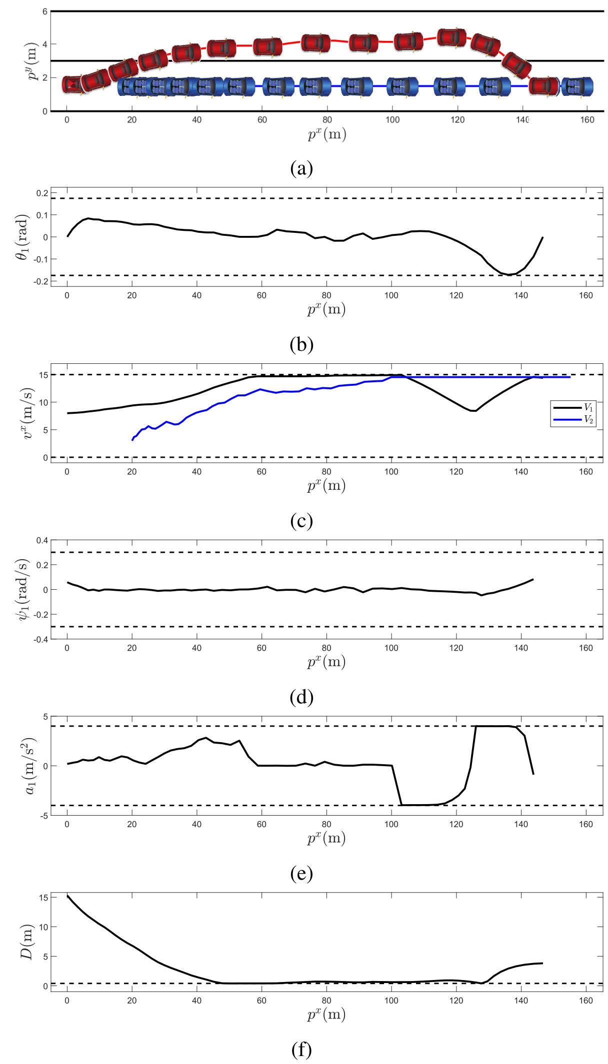

Fig. 10. **Receding horizon control with constant velocity prediction**, second realization: (a) position of two vehicles. (b) Yaw angle of V_1. (c) Longitudinal velocities of two vehicles. (d) Steering angle of V_1. (e) Acceleration of V_1. (f) Distance between two vehicles.

vehicle V_1 performs a lane change. However, due to the significant increase of the longitudinal velocity of V_2, the problem $\hat{\mathcal{P}}$ becomes infeasible when the longitudinal position of V_1 is about 5m. Then, the vehicle V_1 gives up the overtaking attempt and moves back to the previous lane. In Fig. 6(d) and (e), we show that the control inputs of the automated vehicle (steering angle and acceleration) satisfy the control input constraints. Furthermore, Fig. 6(f) shows that the collision avoidance between two vehicles is still guaranteed even though the overtaking attempt fails.

B. Comparison With the Constant Velocity Assumption

We run a Monte Carlo simulation to compare Algorithm 1 with receding horizon control with constant velocity prediction adapted from [5], [7]. We sample 1000 realizations of state trajectories for V_2 with random inputs generated by $\boldsymbol{u}_2(k) = -2 + 6r$ but still guarantee the constraint satisfaction, where r is a uniformly sampled random variable in interval [0, 1]. For the 1000 realizations, we implement Algorithm 1 and receding horizon control with constant velocity prediction.

The simulation results show that the probability of successful overtaking under Algorithm 1 is 89.7%. This is much higher than the 25.3% successful rate under receding horizon control with constant velocity prediction. One explanation for this is that the risk-aware optimal overtaking control takes into account the (partial) reachable sets of V_2 at each time step and such design exhibits more robustness than the control with constant velocity prediction.

Over the 897 successful overtaking scenarios under Algorithm 1, the average computational time at each time step is 2.18 s, where the minimal computational time is 0.87 s and the maximal computational time is 5.62 s. At each time step, the average percent of the total computation time spent on the reachable sets is about 28.4%. Thus, the time for solving the nonlinear programming problem is about 1.56 s. Currently, this computational time is not fast enough for real-time implementation. Thus, to take advantage of the increased success rate of Algorithm 1, an important future work will be to optimize its implementation and evaluate its performance on a realistic hardware platform.

In the following, we detail and compare two realizations. In the first realization, both control methods allow V_1 to safely overtake V_2, as shown in Figs. 7 and 8. We can see that the state, control, and safety constraints are respected in this realization. From Figs. 7(a) and 8(a), we see that our risk-aware optimal overtaking control achieves shorter overtaking distance and time (77.61 m and 6.2 s) than the control with constant velocity prediction, (100.30 m and 9.0 s).

In the second realization, the risk-aware optimal overtaking control achieves successful overtaking as shown in Fig. 9, while the control with constant velocity prediction is unable to perform a safe overtaking before the overtaking becomes infeasible as shown in Fig. 10. In Fig. 9, we show the state and control trajectories, which satisfy the constraints. We can see that V_1 is in front of V_2 when V_2 is at the x-position with 64.34 m. At the same position, however, the vehicle V_1 is still moving in the other lane under the control with constant velocity prediction. Even when the velocity of V_2 reaches the maximal velocity (at about 102.28 m), which implies that overtaking becomes infeasible, V_1 has no chance to merge back and fails to safely overtake V_2. Finally, V_1 gives up overtaking attempt and moves back to the previous lane, as shown in Fig. 10(a).

VII. Conclusion and Future Directions

In this work, we studied the overtaking problem where an automated vehicle tries to overtake another vehicle. Here, we did not require the conventional assumption that the vehicle we want to overtake moves at a constant velocity, which might impose feasibility issues. To increase the possibility of feasible overtaking, we used martingale theory to perform a risk-aware reachability analysis by analytically characterizing the predicted collision probability. We designed a risk-aware optimal overtaking algorithm which can ensure collision avoidance during the whole overtaking process. Finally, we illustrated the effectiveness of the proposed algorithm in a simulated case study and compared our approach to some that has been suggested in the literature.

Future directions of great interest include more efficient methods for solving the optimization problem, the study of the interplay between the automated vehicle and the human-driven vehicle, and experimental evaluation of our approach.

References

[1] P. Koopman and M. Wagner, "Autonomous vehicle safety: An interdisciplinary challenge," *IEEE Intell. Transp. Syst. Mag.*, vol. 9, no. 1, pp. 90–96, Jan. 2017.

[2] S. Dixit *et al.*, "Trajectory planning for autonomous high-speed overtaking using MPC with terminal set constraints," in *Proc. 21st Int. Conf. Intell. Transp. Syst. (ITSC)*, Nov. 2018, pp. 1061–1068.

[3] S. Dixit *et al.*, "Trajectory planning and tracking for autonomous overtaking: State-of-the-art and future prospects," *Annu. Rev. Control*, vol. 45, pp. 76–86, Jan. 2018.

[4] N. Murgovski and J. Sjöberg, "Predictive cruise control with autonomous overtaking," in *Proc. 54th IEEE Conf. Decis. Control (CDC)*, Dec. 2015, pp. 644–649.

[5] J. Karlsson, N. Murgovski, and J. Sjöberg, "Temporal vs. spatial formulation of autonomous overtaking algorithms," in *Proc. IEEE 19th Int. Conf. Intell. Transp. Syst. (ITSC)*, Nov. 2016, pp. 1029–1034.

[6] F. Molinari, N. N. Anh, and L. Del Re, "Efficient mixed integer programming for autonomous overtaking," in *Proc. Amer. Control Conf. (ACC)*, May 2017, pp. 2303–2308.

[7] J. Karlsson, N. Murgovski, and J. Sjöberg, "Computationally efficient autonomous overtaking on highways," *IEEE Trans. Intell. Transp. Syst.*, vol. 21, no. 8, pp. 3169–3183, Aug. 2020.

[8] B. Vanholme, D. Gruyer, B. Lusetti, S. Glaser, and S. Mammar, "Highly automated driving on highways based on legal safety," *IEEE Trans. Intell. Transp. Syst.*, vol. 14, no. 1, pp. 333–347, Mar. 2013.

[9] J. Chen, W. Zhan, and M. Tomizuka, "Autonomous driving motion planning with constrained iterative LQR," *IEEE Trans. Intell. Vehicles*, vol. 4, no. 2, pp. 244–254, Jun. 2019.

[10] A. Raghavan, J. Wei, J. S. Baras, and K. H. Johansson, "Stochastic control formulation of the car overtake problem," *IFAC-PapersOnLine*, vol. 51, no. 9, pp. 124–129, 2018.

[11] J. K. Scott and P. I. Barton, "Bounds on the reachable sets of nonlinear control systems," *Automatica*, vol. 49, no. 1, pp. 93–100, Jan. 2013.

[12] E. Coelingh, L. Jakobsson, H. Lind, and M. Lindman, "Collision warning with auto brake: A real-life safety perspective," in *Proc. 20th Int. Tech. Conf. Enhanced Saf. Vehicles (ESV)*, 2007.

[13] M. Althoff, "Reachability analysis and its application to the safety assessment of autonomous cars," Ph.D. dissertation, Dept. Elect. Eng. Inf. Technol., Technische Univ. München, München, Germany, 2010.

[14] D. P. Bertsekas and I. B. Rhodes, "On the minimax reachability of target sets and target tubes," *Automatica*, vol. 7, no. 2, pp. 233–247, Mar. 1971.

[15] M. Althoff and J. M. Dolan, "Set-based computation of vehicle behaviors for the online verification of autonomous vehicles," in *Proc. 14th Int. IEEE Conf. Intell. Transp. Syst. (ITSC)*, Oct. 2011, pp. 1162–1167.

[16] M. Althoff, O. Stursberg, and M. Buss, "Safety assessment of autonomous cars using verification techniques," in *Proc. Amer. Control Conf.*, Jul. 2007, pp. 4154–4159.

[17] M. Althoff and J. M. Dolan, "Online verification of automated road vehicles using reachability analysis," *IEEE Trans. Robot.*, vol. 30, no. 4, pp. 903–918, Aug. 2014.

[18] K. Leung *et al.*, "On infusing reachability-based safety assurance within planning frameworks for human–robot vehicle interactions," *Int. J. Robot. Res.*, vol. 39, nos. 10–11, pp. 1326–1345, 2020.

[19] A. Abate, M. Prandini, J. Lygeros, and S. Sastry, "Automatica probabilistic reachability and safety for controlled discrete time stochastic," *Automatica*, vol. 44, no. 11, pp. 2724–2734, 2008.

[20] M. Althoff, O. Stursberg, and M. Buss, "Model-based probabilistic collision detection in autonomous driving," *IEEE Trans. Intell. Transp. Syst.*, vol. 10, no. 2, pp. 299–310, Jun. 2009.

[21] D. Sadigh, N. Landolfi, S. S. Sastry, S. A. Seshia, and A. D. Dragan, "Planning for cars that coordinate with people: Leveraging effects on human actions for planning and active information gathering over human internal state," *Auton. Robots*, vol. 42, no. 7, pp. 1405–1426, Oct. 2018.

[22] P. Abbeel and A. Y. Ng, "Apprenticeship learning via inverse reinforcement learning," in *Proc. 21st Int. Conf. Mach. Learn.*, 2004, p. 1.

[23] K. Driggs-Campbell, R. Dong, and R. Bajcsy, "Robust, informative human-in-the-loop predictions via empirical reachable sets," *IEEE Trans. Intell. Vehicles*, vol. 3, no. 3, pp. 300–309, Sep. 2018.

[24] Y. Gao, F. J. Jiang, K. H. Johansson, and L. Xie, "Stochastic modeling and optimal control for automated overtaking," in *Proc. IEEE 58th Conf. Decis. Control (CDC)*, Dec. 2019, pp. 1273–1278.

[25] D. Duffie, *Dynamic Asset Pricing Theory*. Princeton, NJ, USA: Princeton Univ. Press, 2010.

[26] M. H. A. Davis, "Martingale methods in stochastic control," in *Stochastic Control Theory and Stochastic Differential Systems*. Berlin, Germany: Springer, 1979, pp. 85–117.

[27] R. J. Elliott and D. B. Madan, "A discrete time equivalent martingale measure," *Math. Finance*, vol. 8, no. 2, pp. 127–152, Apr. 1998.

[28] Z. Feinstein and B. Rudloff, "A supermartingale relation for multivariate risk measures," *Quant. Finance*, vol. 18, no. 12, pp. 1971–1990, Dec. 2018.

[29] D. Williams, *Probability With Martingales*. Cambridge, U.K.: Cambridge Univ. Press, 1991.

[30] F. Chung and L. Lu, "Concentration inequalities and martingale inequalities: A survey," *Internet Math.*, vol. 3, no. 1, pp. 79–127, Jan. 2006.

[31] X. Zhang, A. Liniger, and F. Borrelli, "Optimization-based collision avoidance," *IEEE Trans. Control Syst. Technol.*, vol. 29, no. 3, pp. 972–983, May 2021.

[32] A. Quimby, G. Maycock, C. Palmer, and S. Buttress, "The factors that influence a driver's choice of speed: A questionnaire study," Transp. Res. Lab., Crowthorne, U.K., Tech. Rep. 325, 1999.

[33] R. Sharma, M. Gupta, and G. Kapoor, "Some better bound on variance with applications," *J. Math. Inequalities*, vol. 4, no. 3, pp. 355–363, 2010.

[34] Y. Nie, O. Faqir, and E. C. Kerrigan, "ICLOCS2: Solve your optimal control problems with less pain," in *Proc. 6th IFAC Conf. Nonlinear Model Predictive Control*, 2018, pp. 2405–8963.

[35] A. Wächter and L. T. Biegler, "On the implementation of an interior-point filter line-search algorithm for large-scale nonlinear programming," *Math. Program.*, vol. 106, no. 1, pp. 25–57, May 2006.

[36] M. Herceg, M. Kvasnica, C. N. Jones, and M. Morari, "Multi-parametric toolbox 3.0," in *Proc. Eur. Control Conf. (ECC)*, Jul. 2013, pp. 502–510.

Yulong Gao received the B.E. degree in automation and the M.E. degree in control science and engineering from Beijing Institute of Technology, Beijing, China, in 2013 and 2016, respectively, and the joint Ph.D. degree in electrical engineering from KTH Royal Institute of Technology, Stockholm, Sweden, and Nanyang Technological University, Singapore, in 2021.

He was a Visiting Student with the Department of Computer Science, University of Oxford, Oxford, U.K., in 2019. He is currently a Post-Doctoral Researcher with the KTH Royal Institute of Technology. His research interests include automatic verification, stochastic control and model predictive control with application to safety-critical systems.

Frank J. Jiang received the B.S. degree in electrical engineering and computer science from the University of California at Berkeley, Berkeley, CA, USA, in 2016, and the M.S. degree in systems, control and robotics from the KTH Royal Institute of Technology, Stockholm, Sweden, in 2019, where he is currently pursuing the Ph.D. degree with the Division of Decision and Control Systems.

His research interests are in formal verification, machine learning, and control, and their applications in robotics and intelligent transportation systems.

Lihua Xie (Fellow, IEEE) received the B.E. and M.E. degrees in electrical engineering from Nanjing University of Science and Technology, Nanjing, China, in 1983 and 1986, respectively, and the Ph.D. degree in electrical engineering from the University of Newcastle, Callaghan NSW, Australia, in 1992.

Since 1992, he has been with the School of Electrical and Electronic Engineering, Nanyang Technological University, Singapore, where he is currently a Professor and Director, Delta-NTU Corporate Laboratory for Cyber-Physical Systems. He held a Teaching Appointments with the Department of Automatic Control, Nanjing University of Science and Technology, from 1986 to 1989. He served as the Head of Division of Control and Instrumentation from July 2011 to June 2014. His research interests include robust control and estimation, networked control systems, multiagent networks, localization, and unmanned systems.

Dr. Xie is a fellow of IFAC and a fellow of Academy of Engineering Singapore. He was an IEEE Distinguished Lecturer from January 2012 to December 2014 and an Elected Member of Board of Governors, IEEE Control System Society from January 2016 to December 2018. He is an Editor-in-Chief for Unmanned Systems and an Associate Editor for the IEEE TRANSACTIONS ON NETWORK CONTROL SYSTEMS. He has served as an Editor of IET Book Series in Control and an Associate Editor of a number of journals including the IEEE TRANSACTIONS ON AUTOMATIC CONTROL, *Automatica*, the IEEE TRANSACTIONS ON CONTROL SYSTEMS TECHNOLOGY, and the IEEE TRANSACTIONS ON CIRCUITS AND SYSTEMS-II.

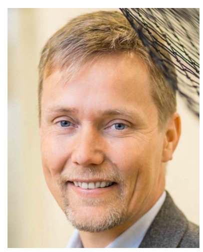

Karl Henrik Johansson (Fellow, IEEE) received the M.Sc. and Ph.D. degrees in electrical engineering from Lund University, Lund, Sweden, in 1992 and 1997, respectively.

He has held a Visiting Positions with the University of California at Berkeley, Berkeley, CA, USA, California Institute of Technology, Pasadena, CA, Nanyang Technological University, Singapore, HKUST Institute of Advanced Studies, Hong Kong, and Norwegian University of Science and Technology, Trondheim, Norway. He is a Professor with the School of Electrical Engineering and Computer Science, KTH Royal Institute of Technology, Stockholm, Sweden, and the Director of Digital Futures. His research interests include networked control systems, cyber-physical systems, and applications in transportation, energy, and automation.

Dr. Johansson is a fellow of the Royal Swedish Academy of Engineering Sciences. He has served on the IEEE Control Systems Society Board of Governors, the IFAC Executive Board, and is currently Vice-President of the European Control Association Council. He has received several best paper awards and other distinctions. He has been awarded Distinguished Professor with the Swedish Research Council and Wallenberg Scholar. He was a recipient of the Future Research Leader Award from the Swedish Foundation for Strategic Research and the triennial Young Author Prize from IFAC. He is an IEEE Distinguished Lecturer.